Supplementary Information for

Real-time visualisation of the intracellular dynamics of conjugative plasmid transfer

Agathe Couturier[a], Chloé Virolle[a], Kelly Goldlust[a], Annick Berne-Dedieu[a], Audrey Reuter[a], Sophie Nolivos[a], Yoshiharu Yamaichi[b], Sarah Bigot[a]* and Christian Lesterlin[a]*

* Corresponding author: Christian.lesterlin@ibcp.fr, Sarah.Bigot@ibcp.fr

This file includes:

Figures S1 to S7
Tables S1 to S3

Other Supplementary Information for this manuscript include the following:

Movies S1 to S3

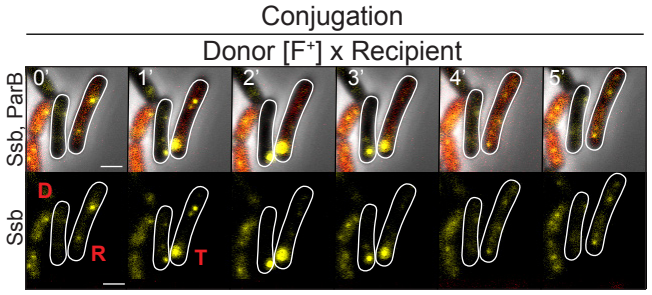
Conjugation
Donor [F+] x Recipient
Ssb, ParB
Ssb
0'
1'
2'
3'
4'
5'
D
R
T

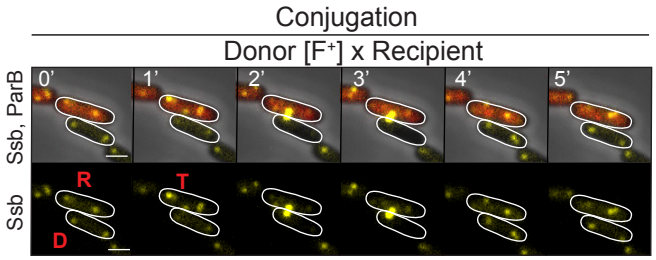
Conjugation
Donor [F+] x Recipient
Ssb, ParB
Ssb
0'
1'
2'
3'
4'
5'
R
T
D

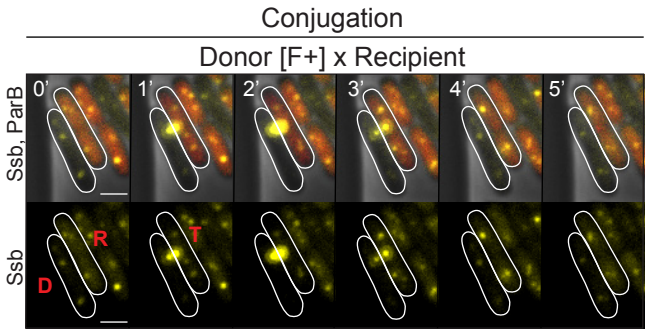
Conjugation
Donor [F+] x Recipient
Ssb, ParB
Ssb
0'
1'
2'
3'
4'
5'
R
T
D

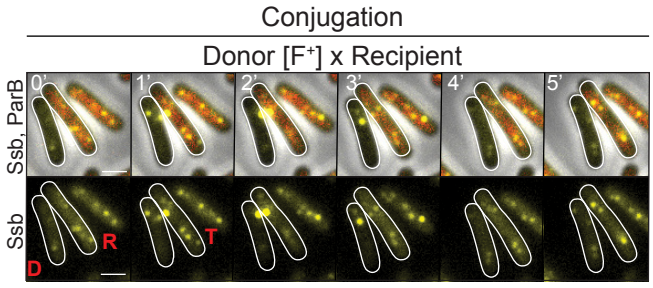
Conjugation
Donor [F+] x Recipient
Ssb, ParB
Ssb
0'
1'
2'
3'
4'
5'
R
T
D

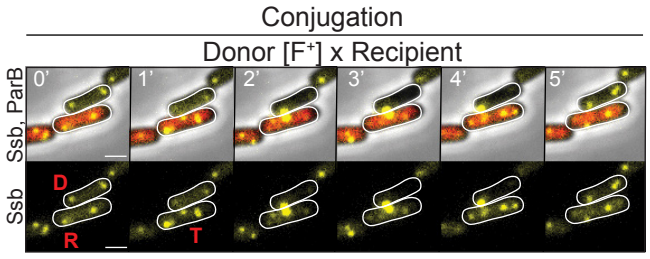
Conjugation
Donor [F+] x Recipient
Ssb, ParB
Ssb
0'
1'
2'
3'
4'
5'
D
R
T

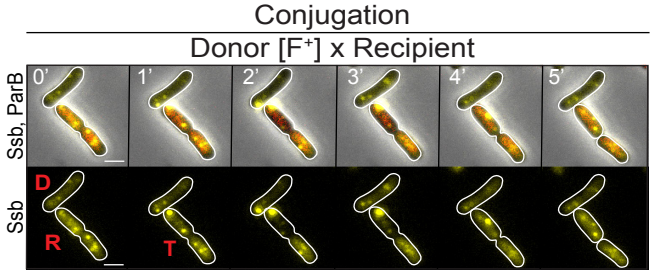
Conjugation
Donor [F+] x Recipient
Ssb, ParB
Ssb
0'
1'
2'
3'
4'
5'
D
R
T

Figure S1. ssDNA transfer events reported by the formation of Ssb-Ypet conjugative foci. Time-lapse microscopy images of conjugation performed in microfluidic chamber showing a plasmid transfer event between a donor (D) and a recipient cell (R) that is converted into a transconjugant (T) (similar to Figure 1b). The transfer of the ssDNA plasmid is reported by the formation of paired bright membrane-associated Ssb-Ypet conjugative foci in both the donor and the transconjugant cell. The recipient cells also produce mCh-ParB. Scale bars 1μm. Donor (LY1007), recipient (LY358), transconjugant (LY358 after F*wt* acquisition from LY1007).

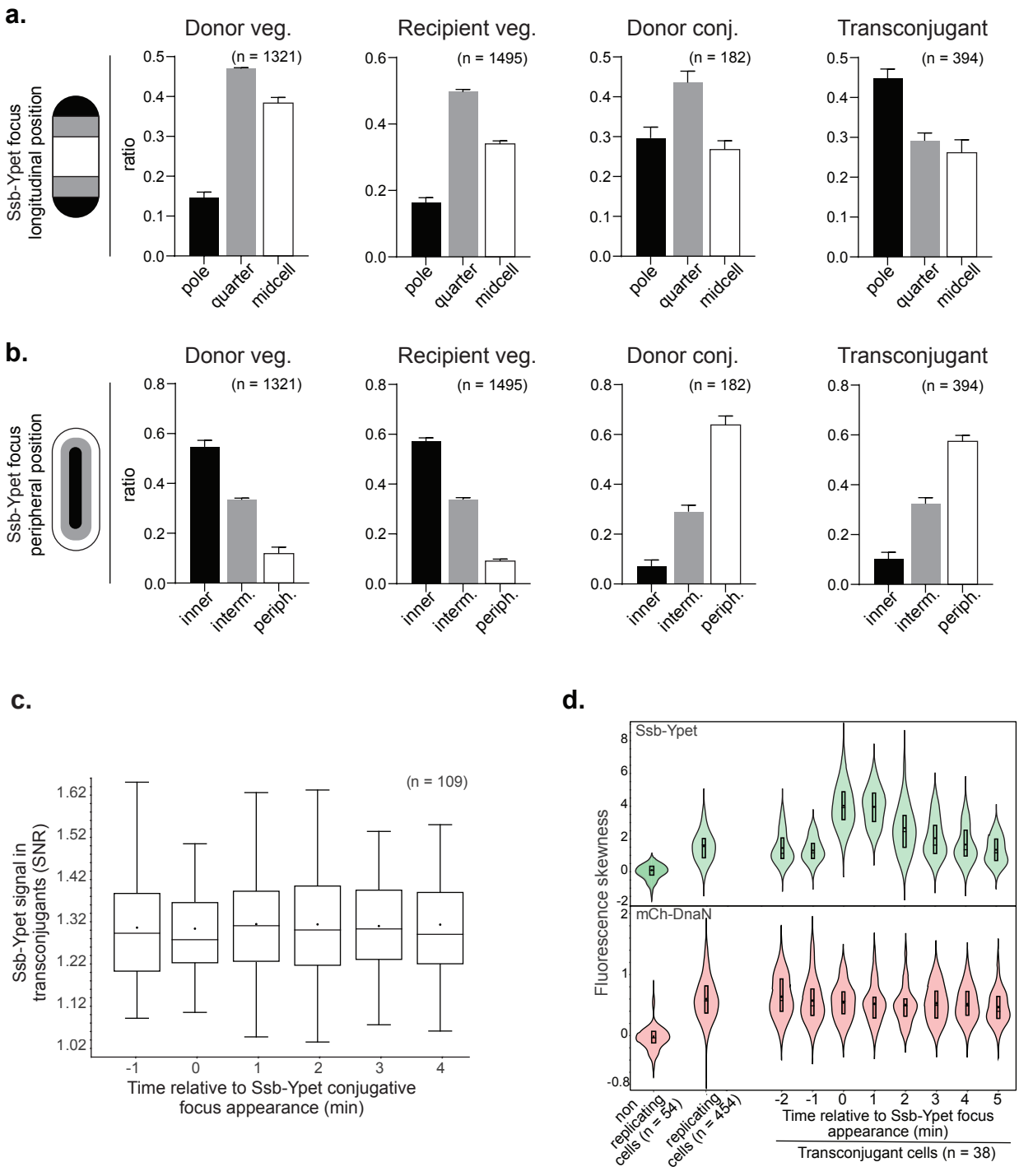
a.
Donor veg.
Recipient veg.
Donor conj.
Transconjugant
Ssb-Ypet focus longitudinal position
ratio
(n = 1321)
(n = 1495)
(n = 182)
(n = 394)
pole
quarter
midcell
b.
Ssb-Ypet focus peripheral position
inner
interm.
periph.
c.
Ssb-Ypet signal in transconjugants (SNR)
(n = 109)
Time relative to Ssb-Ypet conjugative focus appearance (min)
d.
Ssb-Ypet
mCh-DnaN
Fluorescence skewness
non replicating cells (n = 54)
replicating cells (n = 454)
Time relative to Ssb-Ypet focus appearance (min)
Transconjugant cells (n = 38)

Figure S2. Analysis of Ssb-Ypet foci localisation in donor and recipient cells during vegetative growth or during conjugation.

(**a**) Histograms showing the localisation distribution of Ssb-Ypet foci along the cell length sorted in polar, quarter and midcell categories as depicted on the cell diagram (left). (**b**) Histograms showing the localisation distribution of Ssb-Ypet foci within the cell compartment sorted in inner, intermediate and peripheral (i.e., membrane proximal) categories as depicted on the cell diagram (left). For (**a**) and (**b**), the analysis was performed on the same data set as for Figure 1c-d and 1h. Mean and SD are calculated from (n) cells analysed. F*wt* Donor (LY1007), Recipient (LY358). (**c**) Boxplot showing stable Ssb-Ypet intracellular fluorescence (SNR) in transconjugant cells with respect to the ssDNA transfer initiated at t = 0 min. The median, quartile 1 and quartile 3 are indicated by the boxes' bounds, the mean by a black dot, and the minima and maxima by the whiskers' bounds. The analysis was performed on the same data set than for Figure 1I. The number (n) of transconjugant cells analysed is indicated. Transconjugants (LY358 after F*wt* acquisition from LY1007). (**d**) Violin plot showing the skewness of mCh-DnaN and Ssb-Ypet fluorescence in non-replicating and replicating recipient cells in vegetative growth, and in transconjugants with respect to the ssDNA transfer initiated at t = 0 min, as reflected by Ssb-Ypet skewness increase. The number (n) of cells analysed is indicated. The median, quartile 1 and quartile 3 are indicated by the boxes' bounds, the mean by a black dot, and the minima and maxima by the whiskers' bounds. Recipient (LY355), transconjugants (LY355 after F*wt* acquisition from LY1007).

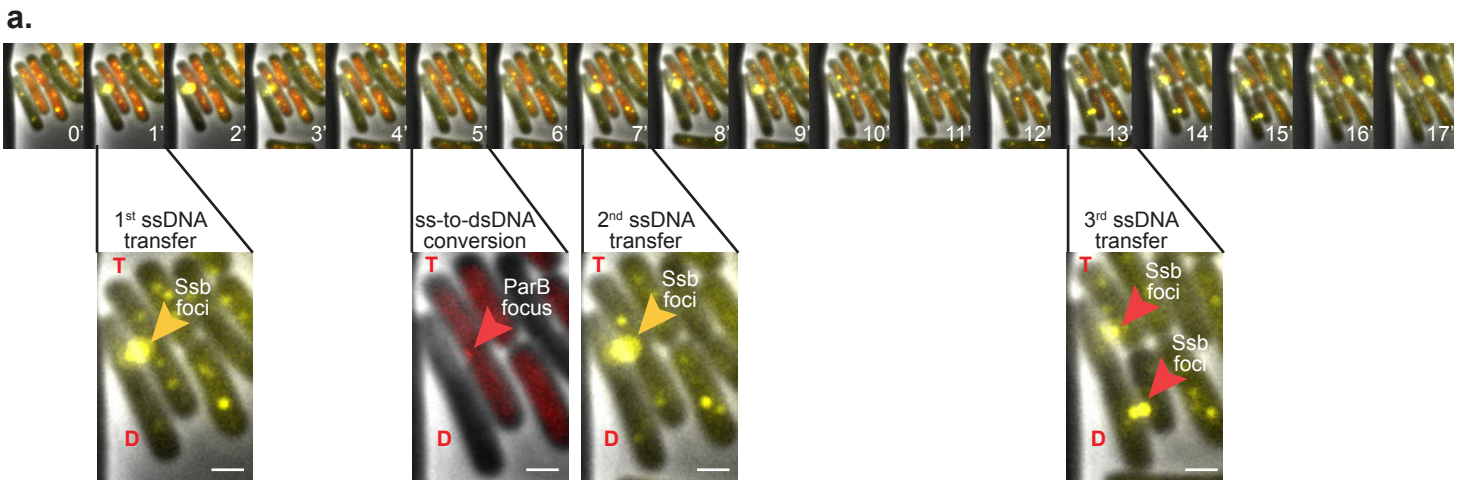
a.
0'
1'
2'
3'
4'
5'
6'
7'
8'
9'
10'
11'
12'
13'
14'
15'
16'
17'
1st ssDNA transfer
ss-to-dsDNA conversion
2nd ssDNA transfer
3rd ssDNA transfer
T
D
Ssb foci
ParB focus

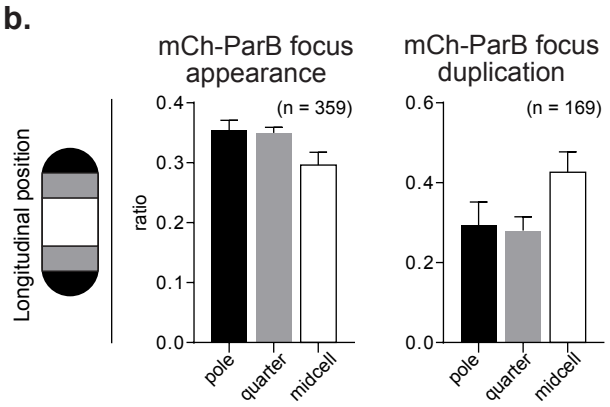
b.
mCh-ParB focus appearance
mCh-ParB focus duplication
(n = 359)
(n = 169)
Longitudinal position
ratio
0.0
0.1
0.2
0.3
0.4
0.6
pole
quarter
midcell

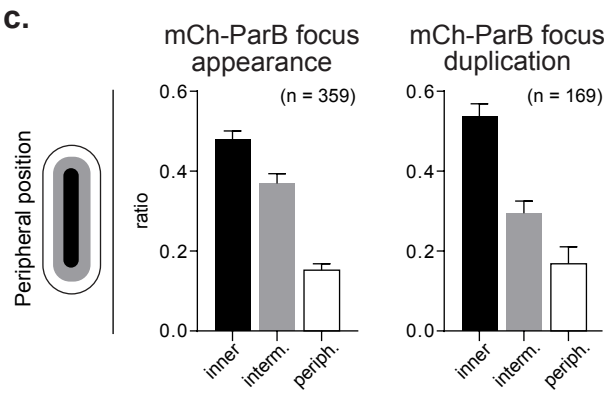
c.
mCh-ParB focus appearance
mCh-ParB focus duplication
(n = 359)
(n = 169)
Peripheral position
ratio
0.0
0.2
0.4
0.6
inner
interm.
periph.

Figure S3. Multiple ssDNA transfer and mCh-ParB localisation analysis.

(**a**) Time lapse microscopy images showing a transconjugant cell that acquires multiple ssDNA plasmids reflected by three consecutive appearances of Ssb-Ypet conjugative foci in both the donor (D) and the transconjugant (T) cells. The transconjugant acquires a first ssDNA plasmid (t=1 min) followed by the appearance of the mCh-ParB focus that reflects the successful ss-to-dsDNA conversion (t=5 min), then a second (t=7 min) and a third (t=13 min) ssDNA plasmid. All three ssDNA come from the same donor cell and appear to occur at the same position along the cell membrane. Scale bars 1μm. (**b**) and (**c**) Histograms showing the localisation distribution of mCh-ParB foci at the time of appearance and just before its duplication into two foci in the transconjugant cells. The analysis was performed on the same data set than for Figure 2H. Mean and SD indicated are calculated from (n) cells analysed from seven independent biological replicates. (**b**) Localisation have been sorted according their polar, quarter and midcell position along the cell length, as depicted on the cell diagram (left). (**c**) Localisation have been sorted according to their inner, intermediate and peripheral (i.e., membrane proximal) positions, as depicted on the cell diagram (left). Donor (LY1007), Recipient (LY358).

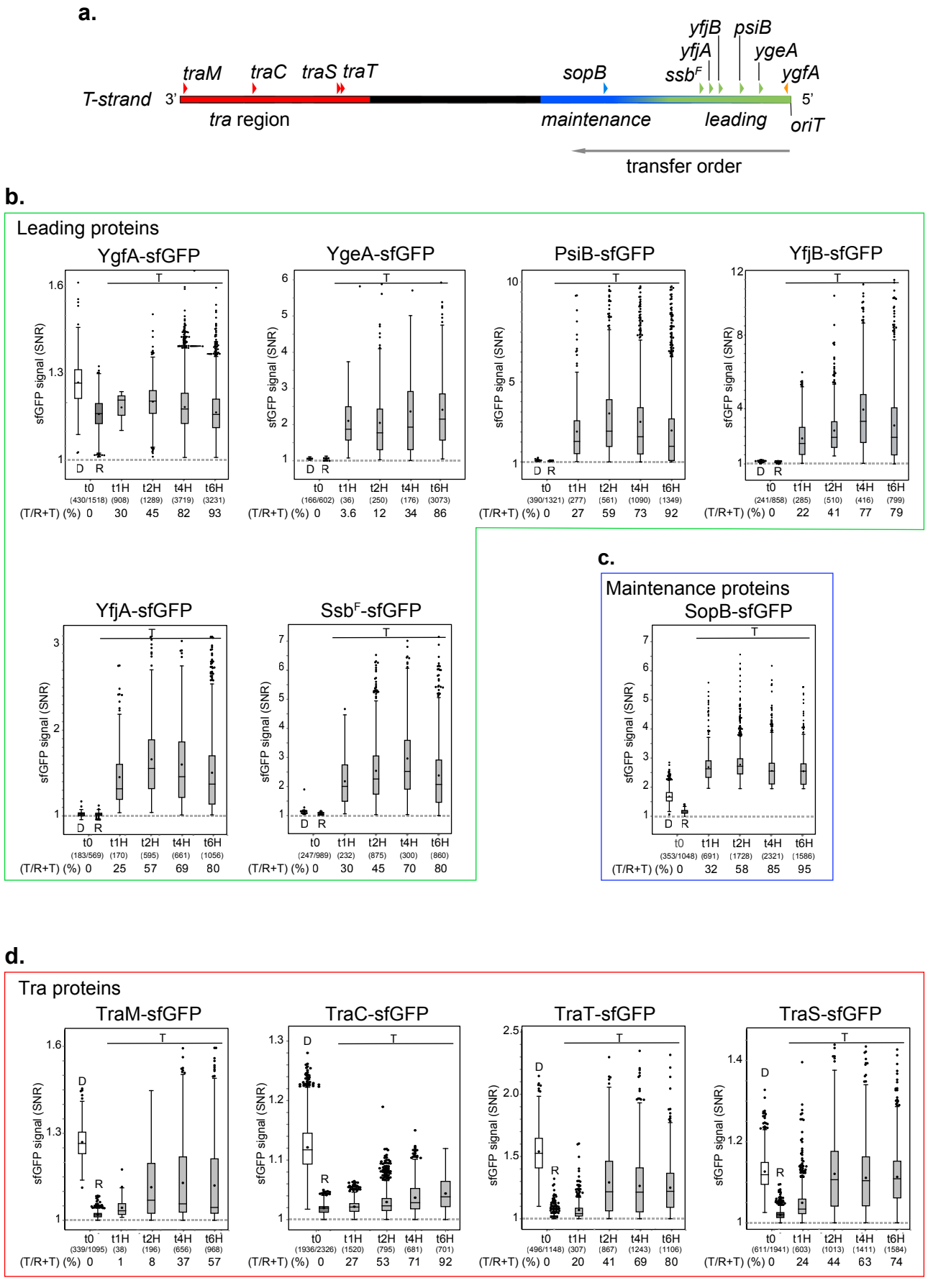
a.
traM
traC
traS traT
T-strand
3'
tra region
sopB
yfjB
psiB
yfjA
ssbF
ygeA
ygfA
5'
oriT
maintenance
leading
transfer order
b.
Leading proteins
YgfA-sfGFP
YgeA-sfGFP
PsiB-sfGFP
YfjB-sfGFP
YfjA-sfGFP
SsbF-sfGFP
sfGFP signal (SNR)
D R
T
t0 t1H t2H t4H t6H
(T/R+T) (%) 0 30 45 82 93
(T/R+T) (%) 0 3.6 12 34 86
(T/R+T) (%) 0 27 59 73 92
(T/R+T) (%) 0 22 41 77 79
(T/R+T) (%) 0 25 57 69 80
(T/R+T) (%) 0 30 45 70 80
c.
Maintenance proteins
SopB-sfGFP
(T/R+T) (%) 0 32 58 85 95
d.
Tra proteins
TraM-sfGFP
TraC-sfGFP
TraT-sfGFP
TraS-sfGFP
(T/R+T) (%) 0 1 8 37 57
(T/R+T) (%) 0 27 53 71 92
(T/R+T) (%) 0 20 41 69 80
(T/R+T) (%) 0 24 44 63 74

Figure S4. Time-course analysis of sfGFP fusion production in transconjugant cells.

(**a**) Genetic map of the F plasmid showing the position, orientation and order of transfer from the *oriT*, of the genes for which C-terminal translational sfGFP fusions have been studied. (**b**), (**c**) and (**d**), box plots showing the quantification of sfGFP fusions intracellular signal (SNR) during conjugation time-course experiments. For each plot, data are presented for donor (D) and recipient (R) cells at t = 0 min, and transconjugant (T) cells at 1, 2, 4 and 6 hours after mixing donors and recipient cells. The median, quartile 1 and quartile 3 are indicated by the boxes' bounds, the mean by a black dot, and the minima and maxima by the whiskers' bounds. Black dots above and below the max and min values correspond to outlier cells. The number of cells analysed (n) from three biological replicates is indicated between brackets, as well as the frequency of transconjugants (T/R+T) directly measured at the single-cell level from the proportion of recipient cells exhibiting diffuse mCh-ParB fluorescence (R) or transconjugant cells harbouring mCh-ParB foci (T). Results are presented for the leading (**b**), maintenance (**c**) and *tra* genes (**d**). Donor (see Table S1), Recipient (LY358).

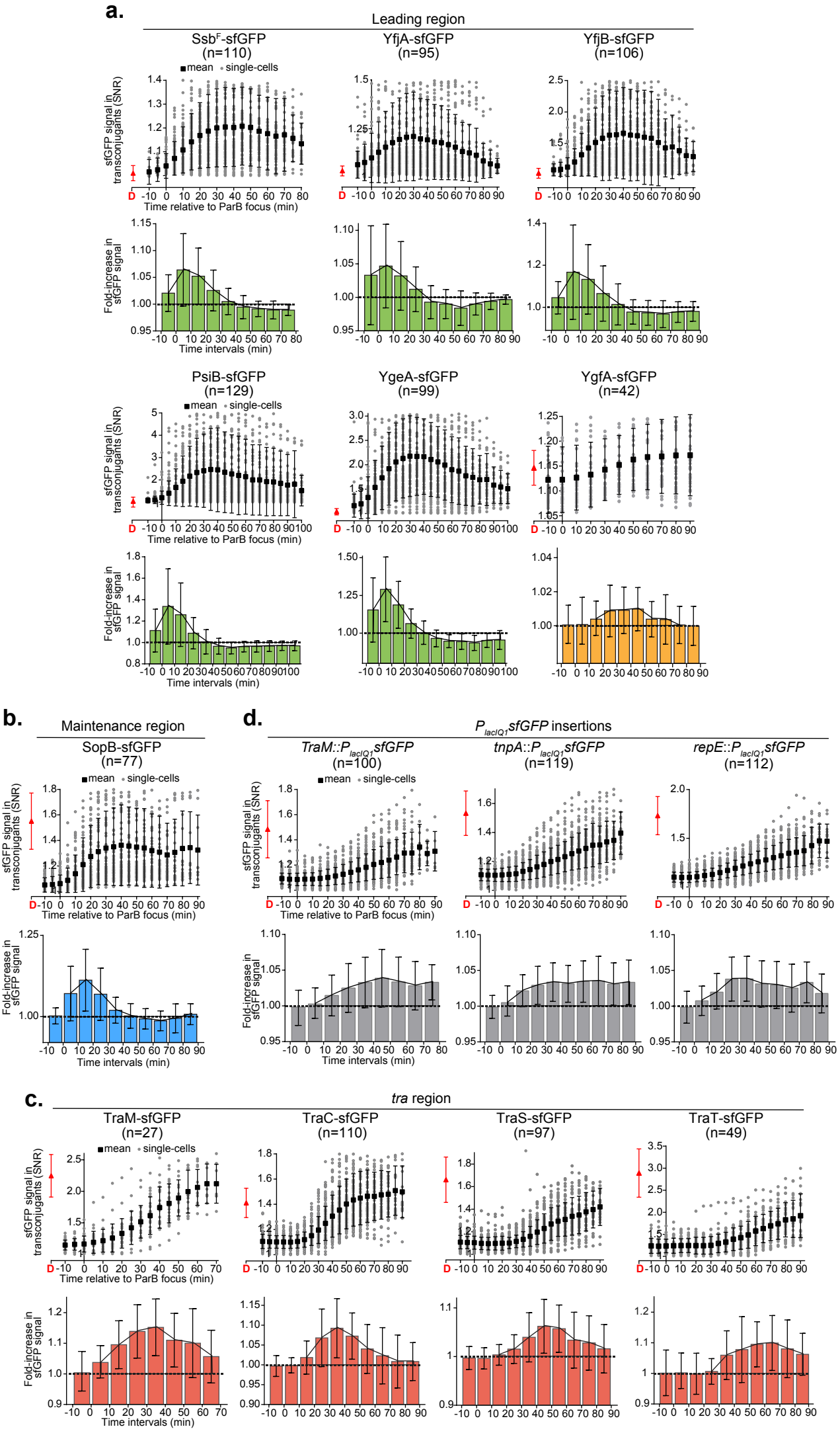
a.
Leading region
SsbF-sfGFP (n=110)
YfjA-sfGFP (n=95)
YfjB-sfGFP (n=106)
PsiB-sfGFP (n=129)
YgeA-sfGFP (n=99)
YgfA-sfGFP (n=42)
mean
single-cells
sfGFP signal in transconjugants (SNR)
Time relative to ParB focus (min)
Fold-increase in sfGFP signal
Time intervals (min)
b.
Maintenance region
SopB-sfGFP (n=77)
d.
PlacIQ1sfGFP insertions
TraM::PlacIQ1sfGFP (n=100)
tnpA::PlacIQ1sfGFP (n=119)
repE::PlacIQ1sfGFP (n=112)
c.
tra region
TraM-sfGFP (n=27)
TraC-sfGFP (n=110)
TraS-sfGFP (n=97)
TraT-sfGFP (n=49)

Figure S5. Time lapse analysis of sfGFP fusion production in transconjugant cells.

(**a-d**) The production level of sfGFP with respect to the appearance of the mCh-ParB focus in individual transconjugant cells was analysed from time lapse microscopy imaging of conjugation performed in microfluidic chambers. Results are presented for the leading (**A**), maintenance (**b**) *tra* genes (**c**), and P_{lacIQ1}sfGFP reporter insertions (**d**). For each fusion, the top panel shows the quantification of sfGFP intracellular signal (SNR) in transconjugant cells over time with respect to mCh-ParB focus appearance (t = 0 min). Each data point representing a single transconjugant cell (grey dots), the Mean (black square) and the SD calculated from the indicated (n) number of cells from at least three independent biological replicates are shown. The Mean and SD observed in donor cells during vegetative growth is also shown (red) for comparison. The bottom panel presents the fold-increase in sfGFP SNR signal by 10 minutes interval calculated from the same data set. Fold-increase >1 reveals the production of sfGFP by the transconjugants in the corresponding time interval. The Mean and SD are indicated. The black polygons show the data that have been used to generate Figure 3b. Donor (see Table S1), Recipient (LY318).

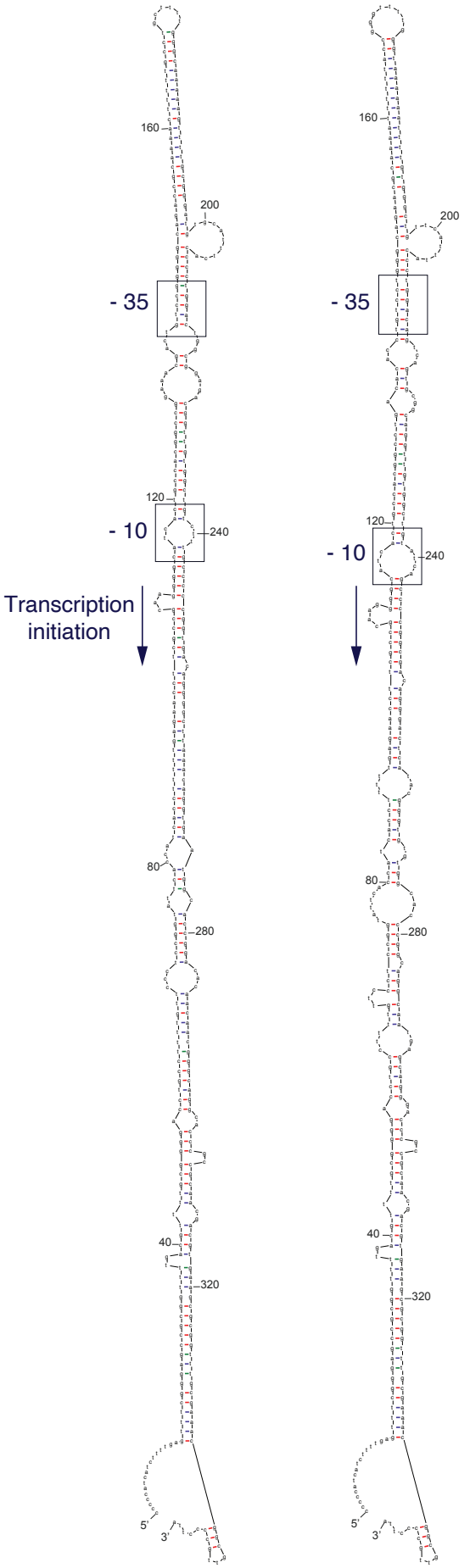

F*rpo1*
dG = -89.22

F*rpo2*
dG = -76.45

Figure S6. F*rpo1* and F*rpo2* stem-loop structure.

Secondary structure folding prediction for F*rpo1* and F*rpo2* sequences in ssDNA forms generated by mFOLD. The reconstructed -35 and -10 boxes are shown (black boxes) with the predicted orientation of transcription initiation. The Gibbs free energy change (dG) indicative of the structure's thermodynamic stability is indicated.

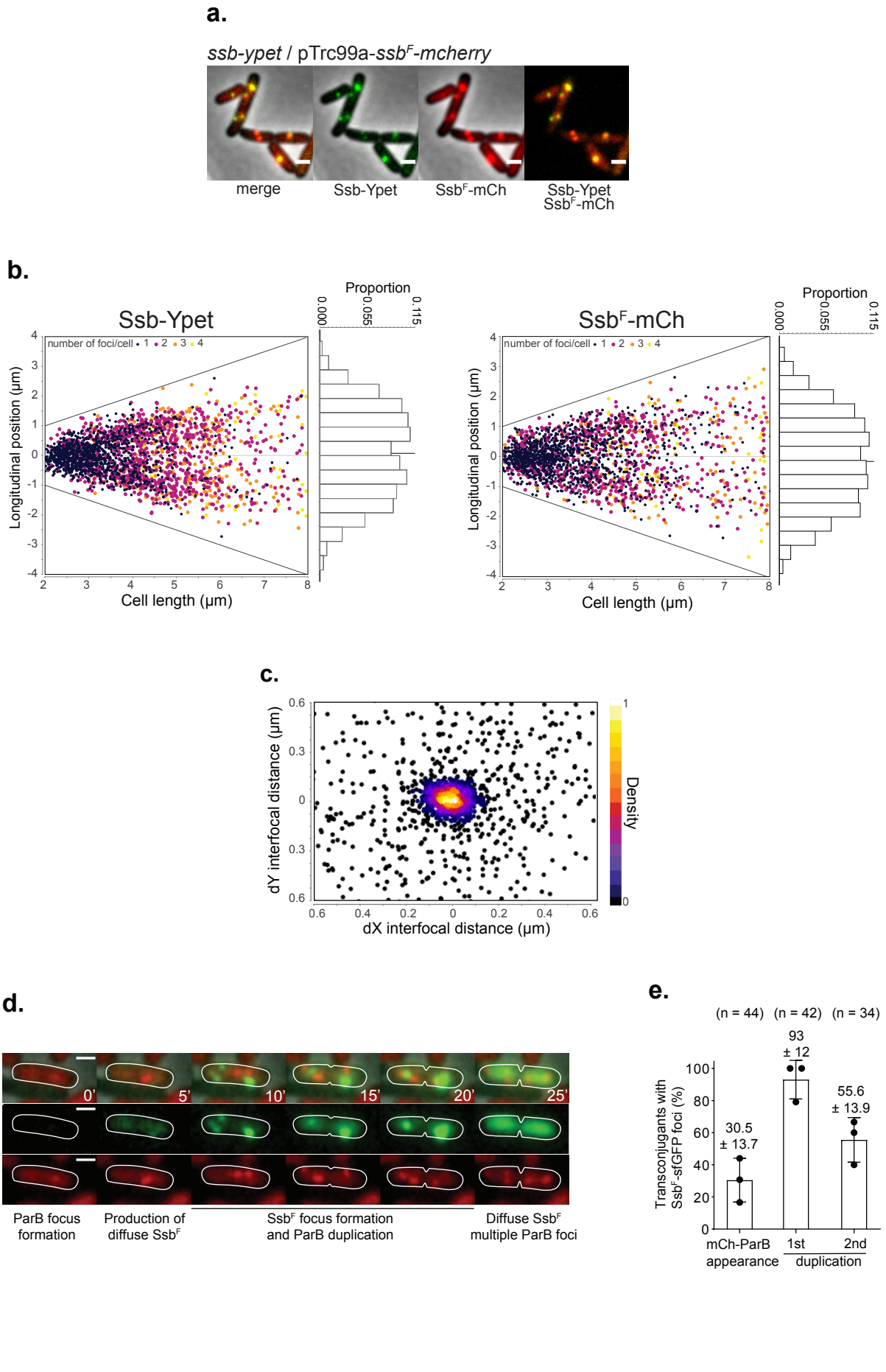
a.
ssb-ypet / pTrc99a-ssbF-mcherry
merge
Ssb-Ypet
SsbF-mCh
Ssb-Ypet
SsbF-mCh
b.
Ssb-Ypet
SsbF-mCh
Proportion
0.000
0.055
0.115
number of foci/cell 1 2 3 4
Longitudinal position (µm)
Cell length (µm)
c.
dY interfocal distance (µm)
dX interfocal distance (µm)
Density
d.
0'
5'
10'
15'
20'
25'
ParB focus formation
Production of diffuse SsbF
SsbF focus formation and ParB duplication
Diffuse SsbF multiple ParB foci
e.
(n = 44) (n = 42) (n = 34)
Transconjugants with SsbF-sfGFP foci (%)
30.5 ± 13.7
93 ± 12
55.6 ± 13.9
mCh-ParB appearance
1st
2nd
duplication

Figure S7. Analysis of Ssb-Ypet and Ssb^F-mCh localisation

(a) Representative microscopy images showing the colocalisation between the chromosomally encoded Ssb-Ypet and Ssb^F-mCh ectopically produced from an expression plasmid during vegetative growth. Scale bars 1μm. Strain LY1382. (**b**) Position analysis of Ssb-Ypet (left) and Ssb^F-mCh (right) foci during vegetative growth presented as localisation dot plots and histogram of distribution along the cell length. (**c**) 2D colocalisation density plot presenting the interfocal distance between Ssb-Ypet and Ssb^F-mCh foci during vegetative growth. The positions of Ssb-Ypet foci are normalised at coordinate (dX = 0, dY = 0) to serve as a localisation reference. The density scale is shown. (**d**) Time lapse microscopy images of conjugation performed in microfluidic chamber showing the formation of mCh-ParB focus (t = 0 min) followed by the production of diffuse Ssb^F-sfGFP (t = 5 min), and formation Ssb^F-sfGFP foci in a transconjugant cell after acquisition of the F *ssb^F-sfgfp* plasmid. Scale bars 1 μm. Transconjugant (LY318 after acquisition of F *ssb^F-sfgfp* from LY270). (**e**) Histograms presenting the proportion of transconjugant cells with Ssb^F-sfGFP foci at the moment of mCh-ParB appearance, first and second duplication events. The mean and SD calculated from the indicated number (n) of transconjugant cells from at least three independent experiments (black dots) are shown.

Strain	Relevant genotype[a, b, c]	Source or reference[a]
MG1655 and derivatives		
LY110	MS388 / F-Tn*10*, *parS$_{PMT1}$-FRT-cat-FRT*	[1]
LY117	MS388 *ssb-ypet-FRT-kan-FRT*	[1]
LY128	MS388 *ssb-ypet-FRT*	[1]
LY159	MS388 / F-Tn*10*, *parS$_{PMT1}$-FRT*, Δ*ygeA::FRT-kan-FRT*	Conjugation LY864 x MS388 to St^R Tc^r
LY160	MS388 / F-Tn*10*, *parS$_{PMT1}$-FRT*, Δ*ygeA::FRT*	Derivative of LY159, kan removed via pCP20
LY240	MS388 / F-Tn*10*, *parS$_{PMT1}$-FRT-cat-FRT*, *ssb^F-sfgfp-FRT-kan-FRT*	Conjugation LY225 x MS388 to St^R Tc^r
LY242	MS388 / F-Tn*10*, *parS$_{PMT1}$-FRT-cat-FRT*, *traM-sfgfp-FRT-kan-FRT*	Conjugation LY227 x MS388 to St^R Tc^r
LY260	MS388 / F-Tn*10*, *parS$_{PMT1}$-FRT-cat-FRT*, *traS-sfgfp-FRT-kan-FRT*	Conjugation LY149 x MS388 to St^R Tc^r
LY261	MS388 / F-Tn*10*, *parS$_{PMT1}$-FRT-cat-FRT*, *traT-sfgfp-FRT-kan-FRT*	Conjugation LY148 x MS388 to St^R Tc^r
LY270	MS388 / F-Tn*10*, *parS$_{PMT1}$-FRT*, *ssb^F-sfgfp-FRT*	Derivative of LY240, cat and kan removed via pCP20
LY272	MS388 / F-Tn*10*, *parS$_{PMT1}$-FRT*, *traM-sfgfp-FRT*	Derivative of LY242, cat and kan removed via pCP20
LY284	MS388 / F-Tn*10*, *parS$_{PMT1}$-FRT-cat-FRT*, *sopB-sfgfp-FRT-kan-FRT*	Conjugation LY276 x MS388 to St^R Tc^r
LY318	MS388 / pSN70	[1]
LY341	MS388 / F-Tn*10*, *parS$_{PMT1}$-FRT-cat-FRT*, *traC-sfgfp-FRT-kan-FRT*	Conjugation LY327 x MS388 to St^R Tc^r
LY355	MS388 *ssb-ypet-FRT*; *mcherry-dnaN-frt-Kan-frt*	Transduction of *mcherry-dnaN-frt-Kan-frt* into LY128 to Km^r
LY358	MS388 *ssb-ypet-FRT* / pSN70	[1]
LY390	MS388 / F-Tn*10*, *parS$_{PMT1}$-FRT-cat-FRT*, *repE::PlacIQ1-sfgfp-FRT-kan-FRT*	[1]
LY728	MS388 / F-Tn*10*, *parS$_{PMT1}$-FRT*, Δ*ssb^F::FRT-kan-FRT*	Conjugation LY718 x MS388 to St^R Tc^r
LY735	MS388 / F-Tn*10*, *parS$_{PMT1}$-FRT*, *yfjB-sfgfp-FRT-kan-FRT*	Conjugation LY731 x MS388 to St^R Tc^r
LY736	MS388 / F-Tn*10*, *parS$_{PMT1}$-FRT*, *yfjA-sfgfp-FRT-kan-FRT*	Conjugation LY733 x MS388 to St^R Tc^r
LY737	MS388 / F-Tn*10*, *parS$_{PMT1}$-FRT*, *ygeA-sfgfp-FRT-kan-FRT*	Conjugation LY732 x MS388 to St^R Tc^r
LY738	MS388 / F-Tn*10*, *parS$_{PMT1}$-FRT*, *psiB-sfgfp-FRT-kan-FRT*	Conjugation LY734 x MS388 to St^R Tc^r
LY754	MS388 / F-Tn*10*, *parS$_{PMT1}$-FRT*, *psiB-sfgfp-FRT*	Derivative of LY738, kan removed via pCP20
LY755	MS388 / F-Tn*10*, *parS$_{PMT1}$-FRT*, Δ*ssb^F::FRT*	Derivative of LY728, kan removed via pCP20
LY756	MS388 / F-Tn*10*, *parS$_{PMT1}$-FRT*, *ygeA-sfgfp-FRT*	Derivative of LY737, kan removed via pCP20
LY791	MS388 / F-Tn*10*, *parS$_{PMT1}$-FRT*, *yfjA-sfgfp-FRT*	Derivative of LY736, kan removed via pCP20
LY792	MS388 / F-Tn*10*, *parS$_{PMT1}$-FRT*, *yfjB-sfgfp-FRT*	Derivative of LY735, kan removed via pCP20

LY803	MS388 / F-Tn*10*, *parS$_{PMT1}$-FRT*, Δ*Frpo1::FRT-kan-FRT*	Conjugation LY795 x MS388 to St^R Tc^r
LY804	MS388 / F-Tn*10*, *parS$_{PMT1}$-FRT*, Δ*Frpo2::FRT-kan-FRT*	Conjugation LY796 x MS388 to St^R Tc^r
LY823	MS388 / F-Tn*10*, *parS$_{PMT1}$-FRT*, Δ*Frpo2::FRT*	Derivative of LY804, kan removed via pCP20
LY824	MS388 / F-Tn*10*, *parS$_{PMT1}$-FRT*, Δ*Frpo1::FRT*	Derivative of LY803, kan removed via pCP20
LY834	MS388 / F-Tn*10*, *parS$_{PMT1}$-FRT*, *sopB-sfgfp-FRT*	Derivative of LY284, cat and kan removed via pCP20
LY875	MS388 / F-Tn*10*, *parS$_{PMT1}$-FRT*,	Conjugation LY162 x MS388 to St^R Tc^r
LY1007	MS388 *ssb-ypet-FRT* / F-Tn*10*, *parS$_{PMT1}$-FRT*	Conjugation LY162 x LY128 to St^R Tc^r
LY1038	MS388 / F-Tn*10*, *parS$_{PMT1}$-FRT*, *ssb^F-mcherry-FRT-kan-FRT*	Conjugation LY1037 x MS388 to St^R Tc^r
LY1053	MS388 / F-Tn*10*, *parS$_{PMT1}$-FRT*, *ssb^F-mcherry-FRT*	Derivative of LY038, kan removed via pCP20
LY1068	MS388 *ssb-ypet-FRT* / F-Tn*10*, *parS$_{PMT1}$-FRT*, Δ*ssb^F::FRT*	Conjugation LY837 x LY128 to St^R Tc^r
LY1149	MS388 / F-Tn*10*, *parS$_{PMT1}$-FRT*, *traC-sfgfp-FRT*	Derivative of LY341, cat and kan removed via pCP20
LY1150	MS388 / F-Tn*10*, *parS$_{PMT1}$-FRT*, *traS-sfgfp-FRT*	Derivative of LY260, cat and kan removed via pCP20
LY1151	MS388 / F-Tn*10*, *parS$_{PMT1}$-FRT*, *traT-sfgfp-FRT*	Derivative of LY261, cat and kan removed via pCP20
LY1216	MS388 / F-Tn*10*, *parS$_{PMT1}$-FRT*, *repE::P$_{lacIQ1}$-sfgfp-FRT*	Derivative of LY390, cat and kan removed via pCP20
LY1224	MS388 / F-Tn*10*, *parS$_{PMT1}$-FRT*, *ygfA-sfgfp-FRT-kan-FRT*	Conjugation LY1219 x MS388 to St^R Tc^r
LY1225	MS388 / F-Tn*10*, *parS$_{PMT1}$-FRT*, *traM::P$_{lacIQ1}$-sfgfp-FRT-kan-FRT*	Conjugation LY1220 x MS388 to St^R Tc^r
LY1226	MS388 / F-Tn*10*, *parS$_{PMT1}$-FRT*, *tnpA::PlacIQ1-sfgfp-FRT-kan-FRT*	Conjugation LY1221 x MS388 to St^R Tc^r
LY1230	MS388 / F-Tn*10*, *parS$_{PMT1}$-FRT*, *ygfA-sfgfp-FRT*	Derivative of LY1224, kan removed via pCP20
LY1231	MS388 / F-Tn*10*, *parS$_{PMT1}$-FRT*, *traM::P$_{lacIQ1}$-sfgfp-FRT*	Derivative of LY1225, kan removed via pCP20
LY1232	MS388 / F-Tn*10*, *parS$_{PMT1}$-FRT*, *tnpA::P$_{lacIQ1}$-sfgfp-FRT*	Derivative of LY1226, kan removed via pCP20
LY1288	MS388 *rpsL* (St^R), *ssb-ypet-FRT*, *dnaE-kan*	P1 LY1158 x LY128 to Kan^R ts
LY1359	MS388 *rpsL* (St^R), *ssb-ypet-FRT*, *polA-tc*	P1 LY1159 x LY128 to Tc^R ts
LY1364	MS388 / F-Tn*10*, *parS$_{PMT1}$-FRT*, Δ*Frpo2::FRT*, *yfjA-sfgfp-FRT-kan-FRT*	Conjugation LY1355 x MS388 to St^R Tc^r
LY1365	MS388 / F-Tn*10*, *parS$_{PMT1}$-FRT*, Δ*Frpo2::FRT*, *ssb^F-sfgfp-FRT-kan-FRT*	Conjugation LY1356 x MS388 to St^R Tc^r
LY1368	MS388 / F-Tn*10*, *parS$_{PMT1}$-FRT*, Δ*Frpo1::FRT*, *ygeA-sfgfp-FRT-kan-FRT*	Conjugation LY1367 x MS388 to St^R Tc^r
LY1373	MS388 *rpsL* (St^R), *ssb-ypet-FRT* / pSN70, clone 1	pSN70 x LY1288 to Ap^r

LY1374	MS388 *rpsL* (St^R), *ssb-ypet-FRT* / pSN70, clone 2	pSN70 x LY1288 to Ap^r
LY1382	MS388 *rpsL* (St^R), *ssb-ypet-FRT* / pAC1	pAC1 x LY128 to Ap^r
LY1418	MS388 / F-Tn*10*, *$parS_{PMT1}$-FRT*, Δ*Frpo1-ygeA::FRT-kan-FRT*	Conjugation LY1414 x MS388 to St^R Tc^r
LY1419	MS388 / F-Tn*10*, *$parS_{PMT1}$-FRT*, Δ*Frpo1-ygeA-ygeB::FRT-kan-FRT*	Conjugation LY1415 x MS388 to St^R Tc^r
LY1424	MS388 / F-Tn*10*, *$parS_{PMT1}$-FRT*, Δ*Frpo1-ygeA::FRT*	Derivative of LY1418, kan removed via pCP20
LY1425	MS388 / F-Tn*10*, *$parS_{PMT1}$-FRT*, Δ*Frpo1-ygeA-ygeB::FRT*	Derivative of LY1419, kan removed via pCP20
LY1737	*MS388 ilva::Pbiofab-mcherry -FRT*	
MG1655	λ^-, *rph-1*	Coli Genetic Stock Center (CGSC) #6300
MS388	MG1655 *rpsL* (St^R)	Gift from F. Cornet
MS428	MG1655 *rpsL* (St^R), ΔlacZ	Gift from F. Cornet
Other genetic backgrounds		
K603	F^+ [F1-10(Tn*10*)], *thr-1, araC14, leuB6*(Am), *lacY1, glnX44*(AS), *galK2*(Oc), *galT22, λ^-, ΔtrpE63, xylA5, mtl-1, thiE1*	Coli Genetic Stock Center CGSC #6451 Strain carrying the F-Tn*10* natural isolate with Tn*10* transposon in the intergenic region *ybdB-ybfA*. GenBank accession number MK492260)
DY330	W3110 Δ*lacU169, gal490, λcI857,* Δ*(cro-bioA)*	[2]
LY183	AB1157 kan-11aa-mcherry-dnaN =	[3]
LY162	DY330 / F-Tn*10-$parS_{PMT1}$-FRT*	[1]
LY148	DY330 / F-Tn*10*, *$parS_{PMT1}$-FRT-cat-FRT, traT-sfgfp-FRT-kan-FRT*	λred *traT-sfgfp* fusion at the endogenous F plasmid *locus* (OL136/OL137)
LY149	DY330 / F-Tn*10*, *$parS_{PMT1}$-FRT-cat-FRT, traS-sfgfp-FRT-kan-FRT*	λred *traS-sfgfp* fusion at the endogenous F plasmid *locus* (OL138/OL139)
LY225	DY330 / F-Tn*10*, *$parS_{PMT1}$-FRT-cat-FRT, ssb^F-sfgfp-FRT-kan-FRT*	λred *ssb^F-sfgfp* fusion at the endogenous F plasmid *locus* (OL25/OL26)
LY227	DY330 / F-Tn*10*, *$parS_{PMT1}$-FRT-cat-FRT, traM-sfgfp-FRT-kan-FRT*	λred *traM-sfgfp* fusion at the endogenous F plasmid *locus* (OL21/OL22)
LY276	DY330 / F-Tn*10*, *$parS_{PMT1}$-FRT-cat-FRT, sopB-sfgfp-FRT-kan-FRT*	λred *sopB-sfgfp* fusion at the endogenous F plasmid *locus* (OL17/OL18)
LY327	DY330 / F-Tn*10*, *$parS_{PMT1}$-FRT-cat-FRT, traC-sfgfp-FRT-kan-FRT*	λred *traC-sfgfp* fusion at the endogenous F plasmid *locus* (OL189/OL190)
LY404	DY330 / F-Tn*10*, *$parS_{PMT1}$-FRT-cat-FRT, repE::P_{lacIQ1}-sfgfp-FRT-kan-FRT*	[1]
LY718	DY330 / F-Tn*10*, *$parS_{PMT1}$-FRT*, Δ*ssb^F::FRT-kan-FRT*	λred Δ*ssb^F::kan* construct at the endogenous F plasmid *locus* (OL194/OL195)
LY731	DY330 / F-Tn*10*, *$parS_{PMT1}$-FRT, yfjB-sfgfp-FRT-kan-FRT*	λred *yfjB-sfgfp* fusion at the endogenous F plasmid *locus* (OL418/OL419)
LY732	DY330 / F-Tn*10*, *$parS_{PMT1}$-FRT, ygeA-sfgfp-FRT-kan-FRT*	λred *ygeA-sfgfp* fusion at the endogenous F plasmid *locus* (OL422/OL423)
LY733	DY330 / F-Tn*10*, *$parS_{PMT1}$-FRT, yfjA-sfgfp-FRT-kan-FRT*	λred *yfjA-sfgfp* fusion at the endogenous F plasmid *locus* (OL415/OL416)
LY734	DY330 / F-Tn*10*, *$parS_{PMT1}$-FRT, psiB-sfgfp-FRT-kan-FRT*	λred *psiB-sfgfp* fusion at the endogenous F plasmid *locus* (OL429/OL430)
LY795	DY330 / F-Tn*10*, *$parS_{PMT1}$-FRT*, Δ*Frpo1::FRT-kan-FRT*	λred Δ*Frpo1 :: kan* construct at the endogenous F plasmid *locus* (OL476/OL477)

LY796	DY330 / F-Tn*10*, *parS$_{PMT1}$-FRT*, Δ*Frpo2::FRT-kan-FRT*	λred Δ*Frpo2 :: kan* construct at the endogenous F plasmid *locus* (OL473/OL474)
LY837	DY330 / F-Tn*10*, *parS$_{PMT1}$-FRT*, Δ*ssB^F::FRT*	Conjugation LY755 x DY330 to St^s Tc^r
LY864	DY330 / F-Tn*10*, *parS$_{PMT1}$-FRT*, Δ*ygeA::FRT-kan-FRT*	λred Δ*ygeA :: kan* construct at the endogenous F plasmid *locus* (OL476/OL508)
LY916	DY330 / F-Tn*10*, *parS$_{PMT1}$-FRT*, Δ*Frpo1::FRT*	Conjugation LY824 x DY330 to St^s Tc^r
LY917	DY330 / F-Tn*10*, *parS$_{PMT1}$-FRT*, Δ*Frpo2::FRT*	Conjugation LY823 x DY330 to St^s Tc^r
LY1037	DY330 / F-Tn*10*, *parS$_{PMT1}$-FRT*, *ssb^F-mcherry-FRT-kan-FRT*	λred *ssb^F-mcherry* fusion at the endogenous F plasmid *locus* (OL92/OL28)
LY1219	DY330 / F-Tn*10*, *parS$_{PMT1}$-FRT*, *ygfA-sfgfp-FRT-kan-FRT*	λred *ygfA-sfgfp* fusion at the endogenous F plasmid *locus* (OL621/OL622)
LY1220	DY330 / F-Tn*10*, *parS$_{PMT1}$-FRT*, *traM::P$_{lacIQ1}$-sfgfp-FRT-kan-FRT*	λred *P$_{lacIQ1}$-sfgfp-FRT-kan-FRT* construct at the F plasmid intergenic *traM locus* (OL114/OL115)
LY1221	DY330 / F-Tn*10*, *parS$_{PMT1}$-FRT*, *tnpA::P$_{lacIQ1}$-sfgfp-FRT-kan-FRT*	λred *P$_{lacIQ1}$-sfgfp-FRT-kan-FRT* construct at the F plasmid intergenic *traM locus* (OL623/OL624)
LY1355	DY330 / F-Tn*10*, *parS$_{PMT1}$-FRT*, Δ*Frpo2::FRT*, *yfjA-sfgfp-FRT-kan-FRT*	λred *yfjA-sfgfp* fusion at the endogenous F plasmid *locus* of LY917 (OL415/OL416)
LY1356	DY330 / F-Tn*10*, *parS$_{PMT1}$-FRT*, Δ*Frpo2::FRT*, *ssb^F-sfgfp-FRT-kan-FRT*	λred *ssb^F-sfgfp* fusion at the endogenous F plasmid *locus* of LY917 (OL25/OL26)
LY1367	DY330 / F-Tn*10*, *parS$_{PMT1}$-FRT*, Δ*Frpo1::FRT*, *ygeA-sfgfp-FRT-kan-FRT*	λred *ygeA-sfgfp* fusion at the endogenous F plasmid *locus* of LY916 (OL422/OL423)
LY1414	DY330 / F-Tn*10*, *parS$_{PMT1}$-FRT*, Δ*Frpo1-ygeA::FRT-kan-FRT*	λred Δ*Frpo1-ygeA :: kan* construct at the endogenous F plasmid *locus* (OL507/OL508)
LY1415	DY330 / F-Tn*10*, *parS$_{PMT1}$-FRT*, Δ*Frpo1-ygeA-ygeB::FRT-kan-FRT*	λred Δ*Frpo1-ygeA-ygeB :: kan* construct at the endogenous F plasmid *locus* (OL476/OL514)

[a] The abbreviations *bla*, *kan and cat* refer to insertions genes conferring resistance to ampicillin (Ap^r) kanamycin (Kn^r), and chloramphenicol (Cm^r); *rpsl* refers to spontaneous mutation conferring resistance to streptomycin. *FRT* refers to the FLP site-specific recombination site.

[b] Tn*10* transposon is located in the intergenic region *ybdB-ybfA* on the F plasmid.

[c] *sfgfp* gene encodes the superfolder Green Fluorescent Protein sfGFP

Table S1. Strains list

Name	Construct and Usage [a]	Source or reference
pCP20	Flp expression plasmid	[4]
p mCherry-*ParB* (pSN70)	IPTG inducible expression of N-terminal fusion mCherry-$ParB_{PMT1}$	[1]
pR6K-sfGFP	Carries *sfgfp-FRT-kan-FRT* used for several C-terminal fusion by λred	[1]
pROD62	Carries *mCherry-FRT-kan-FRT* used for Δ*Frpo1:: kan* and Δ*Frpo2 :: kan* deletion into F-Tn*10*, $parS_{PMT1}$*-FRT* (OL473/OL474, OL476/OL477) by λred and for plasmids construction by Gibson assembly	Gift from R. Reyes-Lamothe, McGill University
pAC1	Carries ssb^F*-mCherry* insertion under P_{trc} promotor on pTrc99a by Gibson assembly (OL608/OL653, OL602/OL603)	Fig. S7
F-Tn*10* conjugative plasmid (from K603) derivatives		
F*wt*	F-Tn*10* with $parS_{PMT1}$ inserted at the intergenic *ygeB-ygfA locus*	[1] Fig. 1-2, 4B, 5B and Fig. S1-3
F ssb^F*-sfgfp*	F-Tn*10* $parS_{PMT1}$ with ssb^F*-sfgfp* translational fusion at the endogenous locus	Fig. 3-4 and Fig. S4-5
F *ygeA-sfgfp*	F-Tn*10* $parS_{PMT1}$ with *ygeA-sfgfp* translational fusion at the endogenous locus	Fig. 3-4 and Fig. S4-5
F *yfjA-sfgfp*	F-Tn*10* $parS_{PMT1}$ with *yfjA-sfgfp* translational fusion at the endogenous locus	Fig. 3-4 and Fig. S4-5
F *yfjB-sfgfp*	F-Tn*10* $parS_{PMT1}$ with *yfjB-sfgfp* translational fusion at the endogenous locus	Fig. 3 and Fig. S4-5
F *psiB-sfgfp*	F-Tn*10* $parS_{PMT1}$ with *psiB-sfgfp* translational fusion at the endogenous locus	Fig. 3 and Fig. S4-5
F *sopB-sfgfp*	F-Tn*10* $parS_{PMT1}$ with *sopB-sfgfp* translational fusion at the endogenous locus	Fig. 3 and Fig. S4-5
F *ygfA-sfgfp*	F-Tn*10* $parS_{PMT1}$ with *ygfA-sfgfp* translational fusion at the endogenous locus	Fig. 3 and Fig. S4-5
F *traM-sfgfp*	F-Tn*10* $parS_{PMT1}$ with *traM-sfgfp* translational fusion at the endogenous locus	Fig. 3 and Fig. S4-5
F *traT-sfgfp*	F-Tn*10* $parS_{PMT1}$ with *traT-sfgfp* translational fusion at the endogenous locus	Fig. 3 and Fig. S4-5
F *traC-sfgfp*	F-Tn*10* $parS_{PMT1}$ with *traC-sfgfp* translational fusion at the endogenous locus	Fig. 3 and Fig. S4-5
F *traS-sfgfp*	F-Tn*10* $parS_{PMT1}$ with *traS-sfgfp* translational fusion at the endogenous locus	Fig. 3 and Fig. S4-5

F *repE*::P_{lacIQ1}-sfGFP	F-Tn*10* $parS_{PMT1}$ with insertion P_{lacIQ1}-*sfgfp* in the *repE-sopA* intergenic region	Fig. 3 and Fig. S5
F *traM*::P_{lacIQ1}-sfGFP	F-Tn*10* $parS_{PMT1}$ with insertion P_{lacIQ1}-*sfgfp* in the *traM-traJ* intergenic region	Fig. 3 and Fig. S5
F *tnpA*::P_{lacIQ1}-sfGFP	F-Tn*10* $parS_{PMT1}$ with insertion P_{lacIQ1}-*sfgfp* in the *tnpA-ybaA* intergenic region	Fig. 3 and Fig. S5
F Δ*Frpo2*	F-Tn*10* $parS_{PMT1}$ with *Frpo2* deletion	Fig. 4B
F Δ*Frpo1*	F-Tn*10* $parS_{PMT1}$ with *Frpo1* deletion	Fig. 4B
F Δ*Frpo2 yfjA-sfgfp*	F-Tn*10* $parS_{PMT1}$ with *yfjA-sfgfp* translational fusion at the endogenous locus and *Frpo2* promotor deletion	Fig. 4 and Fig. S6B
F Δ*Frpo2* ssb^F-*sfgfp*	F-Tn*10* $parS_{PMT1}$ with ssb^F-*sfgfp* translational fusion at the endogenous locus and *Frpo2* promotor deletion	Fig. 4 and Fig. S6B
F Δ*Frpo1 ygeA-sfgfp*	F-Tn*10* $parS_{PMT1}$ with *ygeA-sfgfp* translational fusion at the endogenous locus and *Frpo1* promotor deletion	Fig. 4 and Fig. S6B
F Δssb^F	F-Tn*10* $parS_{PMT1}$ with ssb^F *deletion*	Fig. 4
F Δ*Frpo1* Δ*ygeA*	F-Tn*10* $parS_{PMT1}$ with *Frpo1* and *ygeA* deletions	Fig. 4
F Δ*Frpo1* Δ*ygeAB*	F-Tn*10* $parS_{PMT1}$ with *Frpo1*, *ygeA* and *ygeB* deletions	Fig. 4

[a] *sfgfp* gene encodes the superfolder Green Fluorescent Protein sfGFP

Table S2. Plasmids used in this study

Name	Sequence	Construct
OL1	GTATTGTCACTCATATGATATTTTTGTGTGTG GCCTTCCAGGTCTGCTATGTGGTGCTATCT	λred *parS$_{PMT1}$-FRT-cat-FRT* insertion at the F plasmid intergenic *ygeB-ygfA locus*. PCR on pGBKD3-parS
OL2	ACAGGCATTGTCAGATACCGGTTATGCCGCA AAAGCGGCAGATTGTGTAGGCTGGAGCTGC	
OL17	ATTGAGGCCATTCTTAAGGAACTTGAAAAGC CAGCACCCAGCTCGGCTGGCTCCGCT	λred *sopB-sfgfp* and *sopB-mTurquoise* fusion at the endogenous F plasmid *locus*. PCR on pR6K-sfGFP and pr6K-mTurquoise plasmids.
OL18	TAAGTAAAGACAGATAAACGTAGACTAAAA CGTGGTCGCACATATGAATATCCTCCTTAG	
OL21	ATCTGAGATGGAACGATTTTTTCCAAAAAAT GATGATGAAAGCTCGGCTGGCTCCGCT	λred *traM-sfgfp* fusion at the endogenous F plasmid *locus*. PCR on pR6K-sfGFP plasmid.
OL22	ATCATAAAAACTCTGATATTTGAACGAAGTC AAATTTCGTCATATGAATATCCTCCTTAG	
OL25	GGAGGGTGACGATTACGGGTTTTCAGACGAT ATCCCGTTCAGCTCGGCTGGCTCCGCT	λred *ssb^F-sfgfp* fusion at the endogenous F plasmid *locus*. PCR on pR6K-sfGFP plasmid.
OL26	TGCCCCGCACAGGACGGGGCGGTTGTCACAG TCAGTCGTCATATGAATATCCTCCTTAG	
OL36	TGGTTCTGGCGAATTCGTGTCTAAAGGTGAA GAACTGTTCACCG	pR6K-sfGFP plasmid construct using Gibson assembly. PCR on pROD62 (OL38/OL39) and pKD4-sfGFP (OL36/OL37)
OL37	GCTCCAGCCTACACCCGGGTTATTTGTAGAG CTCATCCAT	
OL38	CCCGGGTGTAGGCTGGAG	
OL39	CACGAATTCGCCAGAACCAGC	
OL114	CCAAAAAATGATGATGAATAAACGAAATTTG ACTTCGTTCCGACTGGAAAGCGGGCAGTG	λred P$_{lacIQ1}$-*sfgfp-FRT-kan-FRT* construct at F plasmid intergenic *traM locus*. PCR on pR6K-sfGFP plasmid
OL115	CGTACTGTCACCTTTTTAAATCATAAAAACTC TGATATTTCATATGAATATCCTCCTTAG	
OL116	ATTTCTTCTTGCGCTGAGCGTAAGAGCTATCT GACAGAACCGACTGGAAAGCGGGCAGTG	λred P$_{lacIQ1}$-*sfgfp-FRT-kan-FRT* construct at F plasmid intergenic *repE-sopA locus*. PCR on pR6K-sfGFP plasmid
OL117	GAGCATAGCGAGCGAACTGGCGAGGAAGCA AAGAAGAACTCATATGAATATCCTCCTTAG	
OL136	TCTCGAAGACCAGCTGGCCAAATCAATCGCA AATATTCTCAGCTCGGCTGGCTCCGC T	λred *traT-sfgfp* fusion at the endogenous F plasmid *locus*. PCR on pR6K-sfGFP plasmid
OL137	GTCAGTCAGGAGGCCGGTCAGACCAGCCTCC GGAAGATAACATATGAATATCCTCCTTAG	
OL138	CAATAGTTACGTCAAAAACAAGAAGTTATCA AGAGTAAAAAGCTCGGCTGGCTCCGCT	λred *traS-sfgfp* fusion at the endogenous F plasmid *locus*. PCR on pR6K-sfGFP plasmid
OL139	GTTTTTTTGTTTTCATCATATATTTACTCTCTA ATATCTTCATATGAATATCCTCCTTAG	
OL189	AGCCTGGCTGGAAGAACATGAGAAATACAG GAGTGTGGCAAGCTCGGCTGGCTCCGCT	λred *traC-sfgfp* fusion at the endogenous F plasmid *locus*. PCR on pR6K-sfGFP plasmid
OL190	GTTCTGCCGTGACGTCGGCGGGTTTCTGCGTT GAACTCATCATATGAATATCCTCCTTAG	
OL194	ATGGGGGCTGAAAACATCAACAGAAGGAGA CACATCGTGTAGGCTGGAGCTGCTTC	λred Δ*ssb^F::kan* construct at the endogenous F plasmid *locus*. PCR on pROD62
OL195	ATGCCCCGCACAGGACGGGGCGGTTGTCACA GTCAGTCGTCATATGAATATCCTCCTTAG	
OL415	CTGGATGAACCATGTCATCCGTGATTTCGGG ATTCTTAAGAGCTCGGCTGGCTCCGCTGC	λred *yfjA-sfgfp* fusion at the endogenous F plasmid *locus*. PCR on pR6K-sfGFP plasmid
OL416	AATGATTGTCTGCCGGACGCGTTCCCGTCCG GCACCTCTCTATCCTCCTTAGTTCCTATT	

OL418	GGATGCCACTGAACGTACCGATAACCTGGCT GATGCCGCCAGCTCGGCTGGCTCCGCTGC	λred *yfjB-sfgfp* fusion at the endogenous F plasmid *locus*. PCR on pR6K-sfGFP plasmid
OL419	TGCTGCCGCCCCGTCTCCGGCGGGGCGGTGT GGTTGTTCATATCCTCCTTAGTTCCTATT	
OL422	TCAGATTAAGCGTGCCGGCCTCGATATCCGG GCGATCTGCAGCTCGGCTGGCTCCGCTGC	λred *ygeA-sfgfp* fusion at the endogenous F plasmid *locus*. PCR on pR6K-sfGFP plasmid
OL423	CAAGATTGCAACAATCAGGAGGGATATTCAT CACATCCGGTATCCTCCTTAGTTCCTATT	
OL429	CGACATCATCCATATCCTGATGGCGGAAGGA GGTCAGGTAAGCTCGGCTGGCTCCGCTGC	λred *psiB-sfgfp* fusion at the endogenous F plasmid *locus*. PCR on pR6K-sfGFP plasmid
OL430	CTGTGCTGAGGGGAACCAGTGCCTGTGAACG TACGCTCATTATCCTCCTTAGTTCCTATT	
OL473	CTTCCTCTTCTTCCTCTTCTTTCCGTTCCTCTC CTGCTTAGTGTAGGCTGGAGCTGCTTC	λred Δ*Frpo2::kan* construct at the endogenous F plasmid *locus*. PCR on pROD62
OL474	TAATGCCACGAACTGCCATGATGTGTCTCCTT CTGTTGATCATATGAATATCCTCCTTAG	
OL476	GCTGCCCTGATTCCTGTCTGTTTTGTTGTTCTC CTGGCAGGTGTAGGCTGGAGCTGCTTC	λred Δ*Frpo1::kan* construct at the endogenous F plasmid *locus*. PCR on pROD62
OL477	TGGATATTTCGGGTACTCATCCTGCTTTCTCC TCTCTCTGCATATGAATATCCTCCTTAG	
OL507	AGATGATGGGGGCTGAAAACCAGAGAGAGG AGAAAGCAGGGTGTAGGCTGGAGCTGCTTC	λred Δ*ygeA::kan* construct at the endogenous F plasmid *locus*. PCR on pROD62
OL508	CAAGATTGCAACAATCAGGAGGGATATTCAT CACATCCGGCATATGAATATCCTCCTTAG	
OL514	TGATAATATAAGTAAAGCCCCGAAATTTTTT CGGGGCTTTACTTATATTACATATGAATATCC TCCTTAG	λred Δ*FrpO-ygeA-ygeB::kan* construct at the endogenous F plasmid *locus*. PCR on pROD62
OL602	GATCCTCTAGAGTCGACCTGCAGGC	pAC1 plasmid construct using Gibson assembly. PCR on pTrc99a (OL602/OL603) and on LY1053 (OL608/OL653)
OL603	CATGGTCTGTTTCCTGTGTGAAATT	
OL608	AACAATTTCACACAGGAAACAGACCATGGCA GTTCGTGGCATTAA	
OL653	GCCTGCAGGTCGACTCTAGAGGATCTTACTT GTACAGCTCGTCCA	
OL621	GAAGAAATCACTTCCGGAAATTAACAGCGTG CAGAACAATAGCTCGGCTGGCTCCGCT	λred *ygfA-sfgfp* fusion at the endogenous F plasmid *locus*. PCR on pR6K-sfGFP plasmid
OL622	GCTTTTGCGGCATAACCGGTATCTGACAATG CCTGTAAGACATATGAATATCCTCCTTAG	
OL623	GGGGGTGACTTGAAGTAAGCCTTATTTTTCTC CTCCTTTGCGACTGGAAAGCGGGCAGTG	λred P_{lacIQ1}-*sfgfp-FRT-kan-FRT* construct at F plasmid intergenic *tnpA locus*. PCR on pR6K-sfGFP plasmid
OL624	GTTTATTGGTATGAAATAAGAAAAAAACCTC CTTTGAATTCATATGAATATCCTCCTTAG	

Table S3. PCR primers used for strain and plasmid constructions